Available online at www.sciencedirect.com
ScienceDirect
Nuclear Physics B (Proc. Suppl.) 190 (2009) 272–277
NUCLEAR PHYSICS B PROCEEDINGS SUPPLEMENTS
www.elsevierphysics.com

Atmospheric Monitoring for the Pierre Auger Observatory

R. Mussa[a] for the Pierre Auger Collaboration [b] *

[a]INFN, Sezione di Torino, Via Pietro Giuria 1, I-10126, Torino, Italy

[b]Pierre Auger Observatory, av. San Martin Norte 304, (5613) Malargüe, Argentina

The monitoring of atmospheric transparency plays a key role in the reconstruction of ultra high energy cosmic rays with the air fluorescence technique. A review of the instruments (LIDARs, Central Laser Facility, Aerosol Phase Function Monitor) for the detection and characterization of cloud and aerosol parameters in the Pierre Auger Observatory is given.

1. Introduction

The Pierre Auger Observatory is the largest facility in the world for the study of ultra-high energy cosmic rays (UHECRs). It is located in Malargüe (69°W 35°S), in the province of Mendoza, Argentina, on a flat highland at about 1400 meters altitude, east of the Andes mountain range. The Observatory is a 'hybrid' facility, as it exploits a dual technique for simultaneous UHECR detection: an array of 1600 water Cherenkov stations (Surface Detector: SD), regularly spaced, covering an area of 3000 km^2, detects air shower particles (muons and electrons) which reach the ground, while a Fluorescence Detector (FD) of 24 UV telescopes, located in four buildings on the edge of the ground array, overlooks the development of the cosmic ray shower through the atmosphere, detecting the fluorescence light emitted by the air molecules at its passage. The estimate of the primary cosmic ray energy done using the FD is based on the reconstruction of the longitudinal profile of the shower. It depends on our ability to reconstruct the actual number of photons emitted at the shower core, from the number of photons observed by the FD telescope. The precise measurement of atmospheric transparency is quite important for this purpose, as we will describe in the next sections.

2. Atmospheric Monitoring of the Observatory

The atmospheric conditions have a dual role in the cosmic ray detection process, as they impact both the formation of the electromagnetic air shower, and the propagation of the shower light. The nitrogen and oxygen molecules have nontrivial effects on the fluorescence yield, and have been discussed by Bohacova [1] at this Conference. Regular launches of radiosondes above the Observatory [2], and ground weather stations, located in the proximity of the FD buildings and in the center of the array, permit to continuously monitor the parameters of molecular atmosphere, such as pressure, temperature, humidity, wind speed and direction. In this paper, we will review the effects of aerosols and clouds on light propagation in the lower part of the atmosphere, called troposphere (from the greek *tropos*=change).

The FD telescopes observe the shower light emitted at a distance x and need to correct for the trasmission of the atmosphere. The number of photons $dN_{FD}(h,z)$ emitted at altitude h and distance z from a given fraction of slant depth dX is related to the number of photons $dN_{em}(h,z)$ observed at the FD entrance window, of area A_{FD}, by the expression:

$$\frac{dN_{FD}(h,z)}{dX} = \frac{dN_{em}(h,z)}{dX} T(h,z) \frac{A_{FD}}{|x|^2} \qquad (1)$$

where $|x|^2 = h^2 + z^2$. For a telescope located at altitude h_{gnd} and a light source at height h and

*mussa@to.infn.it

0920-5632/$ – see front matter
doi:10.1016/j.nuclphysbps.2009.03.099

elevation angle $\varphi = atan(\frac{h-h_{gnd}}{z-z_{FD}})$, the transmission coefficient $T(h,z) = exp(-\tau(h)/sin\varphi)$ where the vertical optical depth (VOD)

$$\tau(h) = \int_{h_{gnd}}^{h} \alpha_{tot}(h')dh' \quad (2)$$

is calculated as the integral of the extinction coefficient $\alpha_{tot} = \alpha_{mol} + \alpha_{aer} + \alpha_{cloud}$.

This contribution mainly focuses on measurements done with techniques using artificial light sources. Subsection 2.1 shows LIDAR measurements of clouds. In subsection 2.2, we describe the two techniques used to calculate the vertical aerosol optical depth (VAOD), which are based on laser beams operating at wavelengths $\lambda = 351{,}355$ nm. In subsections 2.3 and 2.4 we will describe measurements of the angular dependence and of wavelength dependence of aerosol scattering.

2.1. LIDAR measurements on clouds

The monitoring of clouds on the array is performed with two different techniques, using instruments located in the proximity of each FD site. On the roof of each FD building, an infrared cloud camera, described by Anzalone [3] at this conference, takes a full sky mosaic. This is used to extract cloud coverage information for each pixel in the FD field of view and beyond. The main limitation of the IR cameras is the difficulty in measuring cloud height and thickness, as well as multiple cloud layers. Complementary to the cloud cameras, a network of backscattered LIDARs [4], one per FD site, are operated in standalone mode, scanning the atmosphere above each eye, without interfering with FD operation. Each LIDAR station is located at a distance of 150-200 m from the corresponding FD telescope. It is equipped with a pulsed Nd-YLF laser (pulses have λ= 351 nm, 20 ns width, 100 μJ energy, and are shot at 333 Hz repetition rate) and three parabolic mirrors mounted on a steerable frame.

LIDARs perform a hourly sequence of both continuous and discrete sky scans, mostly outside of the FD field of view (FoV). Whenever the LIDARs are required to shoot in the FD field of view the FD data acquisition is vetoed. This happens once per hour, to perform a horizontal set of shots, or just after the occurrence of a very interesting event, to perform a detailed scan (*Shoot the Shower*) of the shower-detector plane, and have a precise characterization of cloud coverage along the line of sight.

The LIDAR backscattered signal is given by the expression:

$$P(r) = P_0 \frac{ct_0}{2} \left(\frac{A_{mirror}}{r^2} \right) \beta(r,\pi) e^{-2\tau(r)} \quad (3)$$

which contains the backscattering coefficient $\beta(r,\pi) = \rho(r)d\sigma(\theta = \pi)/d\Omega$ and the optical depth $\tau(r) = \int_0^r dr' \alpha(r')$.

Every hour, two orthogonal continuous scans are performed, to extract various informations on clouds above each site: cloud coverage, height, optical thickness, number of layers. A typical example of the quality of cloud imaging is shown in Fig.1.

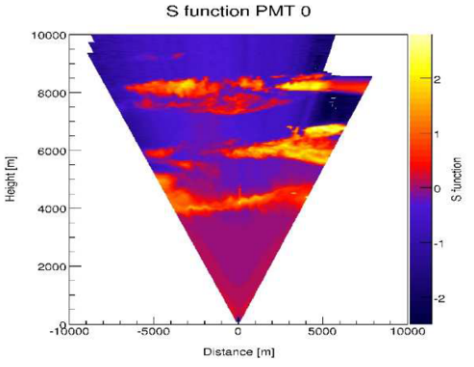

Figure 1. Typical 2D image of clouds above FD site from a continuous LIDAR scan.

An algorithm for differentiating the signals and detecting clouds' edges has been developed. This allows an almost fully automatized analysis and database filling, from LIDAR raw data to cloud database. Summarizing all the data taken during commissioning time, we have that slightly more than 60% of the FD data were taken in almost clear conditions (i.e. with less than 30% of the sky covered by clouds).

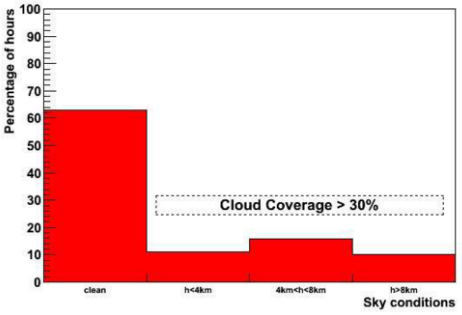

Figure 2. Fraction of nights with cloud coverage above 30% vs cloud height.

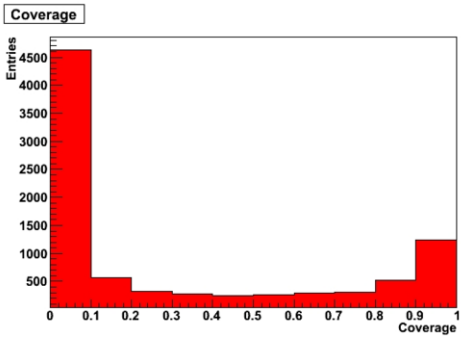

Figure 3. Distribution of cloud coverage.

Fig.2 summarizes the results on cloud coverage versus height and fig.3 the distribution of cloud coverage. It's also important to stress that about 30% of the cloudy hours have multiple layers. In case of thin homogeneous cloud layers, LIDARs can also measure their optical thickness by comparing the power returns, after the correction for the molecular contribution, just below and just above the cloud layer.

2.2. Aerosol Optical Depth measurements

The monitoring of VAOD's is performed by two different laser systems: the Central Laser Facility (CLF), located at the center of the array, which provides regular series of calibrated laser shots to the FD sites [5], and the backscattered LIDAR network described in the previous section. Recently, a new facility (called XLF), has been added at the center of the array, to complement the CLF and provide a better coverage of the northern part of the Observatory. The CLF contains a pulsed ND-YAG laser, frequency triplified, which fires a depolarized beam in hourly sequences (50 shots every 15 minutes) of vertical and inclined pulses, few ns wide, with an energy of about 7 mJ, roughly corresponding to the amount of light generated by a 100 EeV cosmic ray. CLF operations started in late 2003, and 5 full years of data (approximately 5000 hours of VAOD profiles) are now available. XLF operations started in October 2008.

The signal seen by the FD is described by the following equation:

$$P(\varphi_k) = Q_0 \frac{A_{FD}}{R^2} \frac{\beta(h, \pi/2 + \varphi_k)}{1 + tan^2\varphi_k} e^{-\tau(h)(\frac{1+sin\varphi_k}{sin\varphi_k})} \quad (4)$$

known in the literature as bistatic (because source and receiver are not in the same location) LIDAR equation [6]. It is inverted to extract the VAOD(h) profile by comparing $P(\varphi_k)$ with the signal $P_n(\varphi_k)$ observed on a reference night, free of aerosols. The reference signal can be distorted nightly because of changes of the molecular OD profile, of the FD efficiency and PMT gains, of the laser energy calibration: these are the main sources of systematic error of this technique. In coincidence with the laser signal, a light pulse is sent to a close SD unit, that provides relative synchronisation between FD and SD.

Complementary to the CLF/XLF, the LIDAR network, described in previous section, have started operations later on (Coihueco in 2005, Los Morados and Los Leones in fall 2006, and Loma Amarilla in 2008).

LIDAR VAOD extraction does not rely upon the use of a normalization night, and depends on the *a priori* assumption of horizontal homogeneity. It can be shown that the logarithm of the range corrected power return, normalized at con-

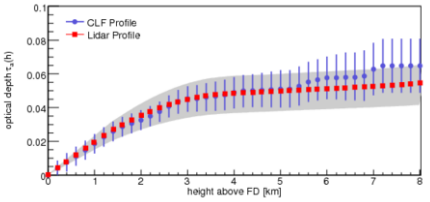

Figure 4. VAOD profiles measured by CLF and LIDAR on a relatively dirty night.

stant height h_n, is a linear function of $sec\theta$, where θ is the polar angle of the LIDAR shot:

$$S(h;h_n) = ln\frac{P(h)h^2}{P(h_n)h_n^2} = ln\frac{\beta(h,\pi)}{\beta(h_n,\pi)} - 2\tau(h_n,h)sec\theta \quad (5)$$

The VAOD between the normalization height h_n and a given height h is therefore given by $\frac{1}{2}\frac{\partial S}{\partial sec\theta}$. Sets of discrete shots at fixed $sec\theta$ values can then be used to decouple from the knowledge of β and invert the LIDAR equation, extracting the VAOD (multiangle inversion [7]). Such procedure cannot be applied below 600-800 m from site, where the laser spot is not completely contained in the LIDAR telescope field of view. This is the main limitation to the current LIDAR system: to overcome it, the aerosol OD is measured at ground with horizontal LIDAR shots, and a constant value of the aerosol content is assumed in the area of incomplete overlap. Figure 4 Hourly VAOD profiles are then written to the experiment database and used in the event reconstruction (see an example in Fig.4, where two profiles taken during the same hour, with systematic error bars, can be compared).

The uniformity of the lower aerosol layers, and of the cloud coverage, is not at all guaranteed on a surface of about 3000 km^2. Local disuniformities due to human activities (land fires) or to natural phenomena (sand and dust blown by the wind, volcanic ashes), can affect VAOD determination as well as shower reconstruction. Work is in progress to quantify the effects of local inhomogeneities in aerosol distributions.

2.3. Aerosol Angular Distribution

In desert areas, aerosols' shapes and sizes can show very large variations, which affect their angular distribution as well as the wavelength dependence. In atmospheric physics, the angular dependence of the scattering is often referred as the phase function $P(\theta)$ given by $P(\theta) = \frac{1}{\sigma}\frac{d\sigma}{d\Omega} = \beta(x,\theta)/\alpha(\theta)$ This applies to both aerosols and molecules, and we can write:

$$\beta = \beta_m + \beta_a = \alpha_m P_m(\theta) + \alpha_a P_a(\theta) \quad (6)$$

The phase function for molecules is described by Rayleigh formula,

$$P_m(\Omega) = \frac{3}{16\pi}(1+\cos^2\theta) \quad (7)$$

while for aerosols there are many approaches: Mie scattering theory [8], devised to describe scattering on hard spheres, is not suited to describe typical aerosols in desert areas. It is more convenient to parametrize the aerosol phase function as given by Henyey and Greenstein[9]:

$$P_a(\theta) = \frac{1-g^2}{4\pi}\left(\frac{1}{(1+g^2-2gcos\theta)^{3/2}}\right) + f\frac{1-g^2}{8\pi}\left(\frac{3cos^2\theta-1}{(1+g^2)^{3/2}}\right) \quad (8)$$

where $g = < cos\theta >$ and f are two empirical parameters.

In the Auger Observatory, two Aerosol Phase Function monitoring stations (APFs) have been installed at a distance of about 1.5 km from the FD sites of Coihueco and Los Morados [10]. Each APF is equipped with a Xenon flash lamp ($\lambda = 350nm$) which shoots a horizontal beam across the FD field of view, few times per hour. These shots, recorded by the FD, allow to measure the differential scattering cross section $d\sigma/d\Omega$ of the atmosphere in front of the FD, for polar angle values ranging from 30 to 150 degrees. The yearly average [11] of the g parameter measured by APFs is $< g >= 0.60 \pm 0.08$, typical of desert areas [12]. The distributions of f and g parameters are shown in Fig.5.

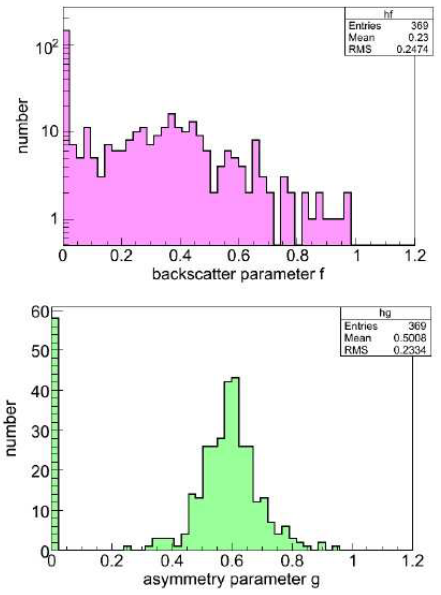

Figure 5. APF results on parameters f and g.

2.4. Wavelength dependence of aerosol cross section

Aerosol scattering properties depend on both size of particulate and wavelength of the incident light. The wavelength dependence of aerosol transmission coefficient is measured by two devices, the Horizontal Attenuation Monitor (HAM) and the Fotometric Robotic telescope for Astronomical Monitoring (FRAM). Both detectors are located at Los Leones, and can measure the wavelength dependence of the intensity of a broadband calibrated light source located on the Coihueco hill. A filter wheel in front of the detector allows to select among 5 wavelengths in the range 350-550 nm. Following Angström [13], the dependence of optical depth on wavelength is usually parametrized as a power law:

$$\tau_a(\lambda) = \tau_0 \left(\frac{\lambda_0}{\lambda} \right)^{\gamma} \qquad (9)$$

where γ is referred to as Angström index. Typically, desert areas are characterized by coarse particulate ($> 1\mu m$), from which we expect little wavelength dependence. HAM data taken in 2006-7 show an average Angström index $\gamma = 0.7 \pm 0.5$. The FRAM is a steerable telescope, and allows to use also the stars as calibrated sources: its results are consistent with HAM ones, but with larger errors.

3. Impact of atmospheric effects on shower reconstruction

The impact of aerosols on shower energy and X_{max} has been estimated on cosmic ray events detected by the Observatory in the period 2005-2008. Hourly data on aerosols on site are taken by CLF, XLF and the four LIDARs and stored in the experiment database. We can then compare the properties of reconstructed showers with and without aerosol corrections, from database or from monthly models. By fully neglecting aerosol corrections, we underestimate shower energies by 8% in average. If we account only for high energy showers (> 10 EeV), the bias increases to 15%, as such showers are observed usually at larger distances, where atmospheric effects become more relevant. Aerosols are responsible for large non gaussian tails in the distributions of energy corrections: 15% of the showers have an energy correction larger than 25%, when we account for the aerosol contribution. In the case of close showers, the energy can also be overestimated, due to the presence of a large contribution from Cherenkov light scattered by aerosol layers.

The angular and wavelength dependence of aerosol contributions is relatively small, and does not produce an energy dependent effect on the reconstruction of shower parameters. Figures 6 and 7 show the effects on energy and X_{max}, as function of the measured energy, if we change the atmospheric parameters by $\pm 1\sigma$.

The impact of clouds on shower reconstruction has been quantified by comparing days with >90% cloud coverage with clear days: a positive bias $\Delta X_{max} = 15 \pm 4 g/cm^2$ has been estimated from the data. No energy dependence on this bias is observed. Another effect of clouds is observed on the flux of hybrid events, which on a year average is underestimated by $17 \pm 5\%$.

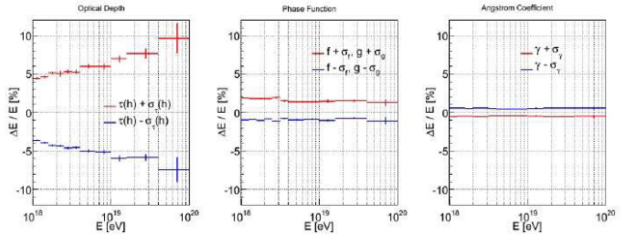

Figure 6. Relative systematic errors on energy from (left to right) VAOD, angular distributions, Angström index, as function of measured energy.

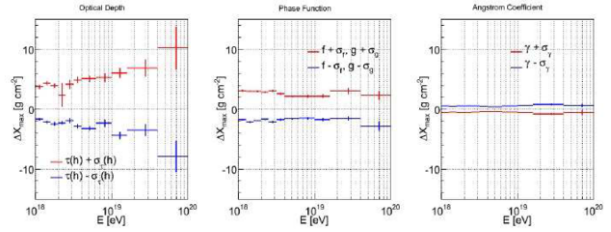

Figure 7. Systematic errors on X_{max} from (left to right) VAOD, angular distributions, Angström index, as function of measured energy.

4. Acknowledgments

The author thanks Antonio Insolia and Rossella Caruso for their kind hospitality, and all the Auger colleagues involved in the atmospheric monitoring task for many fruitful discussions.

REFERENCES

1. M.Bohacova, these Proceedings
2. B.Keilhauer et al., Astropart.Phys.25 (2006),259
3. A.Anzalone, these Proceedings
4. S.Y.BenZvi et al., Nucl.Instr.Meth. A574 (2007),171
5. L.Wiencke, Nucl.Instr.Meth. A572 (2007),508
6. T.D .Stevens, C.R.Philbrick, J.Geophys.Res. 89(D22) (1984),2541
7. A.Filipcic et al., Astropart.Phys. 18 (2003),501
8. G.Mie, Ann.Phys. 25 (1908),377
9. L.G.Henyey, J.L.Greenstein, Astrophys.J.93 (1941),70
10. S.Y.BenZvi et al., Astropart.Phys. 28 (2007),312
11. S.Y.BenZvi et al., Proc.30th ICRC (2007), arXiv:0706.3236
12. E.Andrews et al., J. Geophys. Res. 111 (D10) (2006),D05S04
13. A.Angström, Geographical Analysis 12 (1929),130